Microelectronic Engineering 110 (2013) 311–314

Contents lists available at SciVerse ScienceDirect

Microelectronic Engineering

journal homepage: www.elsevier.com/locate/mee

Deep reactive ion etching of in situ boron doped LPCVD $Ge_{0.7}Si_{0.3}$ using SF_6 and O_2 plasma

S.N.R. Kazmi *, C. Salm, J. Schmitz

MESA+ Institute for Nanotechnology, University of Twente, P.O. Box 217, 7500 AE Enschede, The Netherlands

A R T I C L E I N F O

Article history:
Available online 21 February 2013

Keywords:
Deep reactive ion etching
$Ge_{0.7}Si_{0.3}$
Etch selectivity
Resonator

A B S T R A C T

This paper reports on deep reactive ion etching (DRIE) of in situ highly boron doped low pressure chemical vapor deposited $Ge_{0.7}Si_{0.3}$ alloy in SF_6 and O_2 plasma. The effect of RF power, SF_6 flow, O_2 flow and temperature on the etch rate of $Ge_{0.7}Si_{0.3}$ films with a boron concentration of 2.1×10^{21} atoms/cm^3 is investigated. Optimized conditions for a combination of a vertical etch profile and a high selectivity towards PECVD oxide are reported. The effect of boron doping concentration on the etch rate is also investigated. The etch rate is found to decrease with an increase in the dopant concentration. The developed SF_6 and O_2 based DRIE recipes are applied to fabricate GeSi microresonators.

© 2013 Elsevier B.V. All rights reserved.

1. Introduction

Germanium–silicon (GeSi) alloys have received much attention over the past few decades due to a range of applications; for instance, in heterojunction bipolar transistors [1], MOSFET gates [2] and source/drain regions [3], solar cells [4] and thin film transistors [5]. The application of these layers in CMOS-MEMS post-processing is currently under study [6,7]. Anisotropic etching of the GeSi alloy is necessary in most of these applications.

Dry etching techniques are commonly applied in microtechnology to precisely transfer the desired pattern with a great degree of anisotropicity. A myriad of halogen containing plasma chemistries has been used to demonstrate the dry etching of un-doped GeSi [8–11]. However, to our knowledge, no literature regarding deep reactive ion etching (DRIE) of highly doped GeSi is available; although the experience with highly doped silicon provides a good starting point [12].

In this article, the DRIE of in situ highly boron doped $Ge_{0.7}Si_{0.3}$ layers is described. A mixture of SF_6 and O_2 is chosen for its proven ability to control the anisotropy, as observed in silicon etching [13]. The primary aim of this work is to achieve a vertical etch profile and a good selectivity, at least 50:1 towards SiO_2. We further studied the etch rate as a function of boron concentration in the $Ge_{0.7}Si_{0.3}$ layer. The optimized etch recipes are applied in the fabrication of micromechanical resonators.

2. Experimental

The starting material were 100-mm ⟨1 0 0⟩ oriented Si wafers covered with 100 nm SiO_2 deposited by PECVD (plasma-enhanced chemical vapor deposition). On top of this a 1.5 μm thick in situ boron doped $Ge_{0.7}Si_{0.3}$ films was deposited by means of LPCVD (low-pressure chemical vapor deposition) using SiH_4, GeH_4, Ar and B_2H_6 as gaseous precursors. The $Ge_{0.7}Si_{0.3}$ films were deposited at a temperature of 430 °C and total pressure of 0.2 mbar. The heavily doped films used in this work have a boron concentration of 2.1×10^{21} atoms/cm^3 as determined by SIMS. For comparison also the etch rate is studied for un-doped films and in situ-doped GeSi layers with a lower boron concentration. In this case the boron concentration in the films was varied by changing the ratio of the partial pressures of the gasses, keeping the Si to Ge ratio in the deposited films constant within 2%. More information on the fabrication of the samples can be found in Ref. [14]. Before patterning, the wafers were cleaned in 99% fuming nitric acid for 5 min followed by deionized water rinse and nitrogen drying. The patterning was done by means of optical lithography after spinning and prebaking 1.2 μm Olin 907-12 photoresist at 95 °C for 1 min (without post-bake). The GeSi native oxide was removed by dipping the samples in 1% HF immediately before loading into the etcher to avoid etch inhibition [15].

All etch experiments were performed in a Plasmalab100 Plus system from Oxford Instruments, having a quartz dome, as shown in Fig. 1. The vacuum chamber has a process window of 6–33 $\times 10^{-3}$ mbar pressure and 10–200 sccm flow. The reactor has two power controlled plasma sources. The first is an inductively coupled plasma (ICP) source having a helicoil design to create a high radical and ion density of maximum 1200 W at 13.56 MHz. The second is a capacitively coupled CCP source of maximum 300 W also at 13.56 MHz; it can be used to direct the ions from the plasma glow region towards the wafer surface. The wafer was mechanically clamped against a liquid nitrogen cooled electrode, with helium backside cooling to allow optimum

* Corresponding author. Tel.: +31 53 489 2645; fax: +31 53 489 1034.
E-mail address: snrkazmi@gmail.com (S.N.R. Kazmi).

0167-9317/$ - see front matter © 2013 Elsevier B.V. All rights reserved.
http://dx.doi.org/10.1016/j.mee.2013.02.034

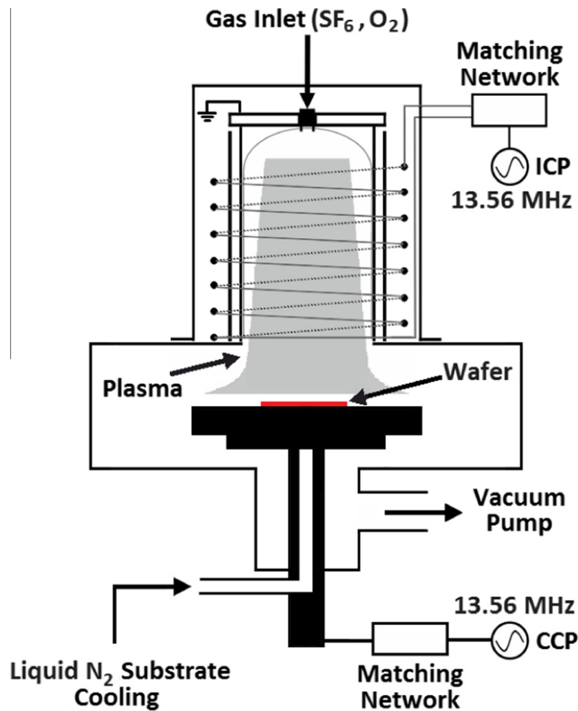

Fig. 1. Schematic layout of the Oxford Plasmalab 100 Plus system.

temperature control over the entire wafer surface. The gases were injected from the top into the process chamber through a gas inlet.

Prior to performing the etching experiments the chamber is cleaned with a 20 min O_2 plasma at 20 °C, to minimize the etch variability [16,17]. The gas flows and process pressure were allowed to stabilize for 5 min before the etching was performed.

The chamber pressure, helium backside pressure and CCP power were kept fixed at 13×10^{-3} mbar, 20 mbar and 10 W, respectively. At the low CCP power of 10 W, corresponding to a self bias of ~20 eV, a high selectivity to the mask is guaranteed. To optimize the GeSi etch the ICP power was varied from 0 to 800 W, the SF_6 flow was varied between 0 and 200 sccm, the O_2 flow was varied between 2 and 20 sccm and the chuck temperature ranged between −110 and 20 °C. In all figures the O_2 flow is excluding the approximately 10% additional oxygen due to the quartz dome. The effects of loading and selectivity towards of photoresist were not studied in this work.

The etch depth and hence the etch rate of highly doped $Ge_{0.7}Si_{0.3}$ was determined using a Dektak 8.0 surface profilometer after removing the photoresist. The etch profile was evaluated from cross-section scanning electron microscopic (SEM) images.

Secondary Ion Mass Spectroscopy (SIMS) was carried out to determine the boron concentration in the deposited $Ge_{0.7}Si_{0.3}$ layers. The SIMS analysis was performed using 3 keV O_2^+ primary ions in positive mode.

3. Results and discussion

The chamber pressure of 13×10^{-3} mbar yields a relatively large mean free path of the reactive species while passing through the dark sheath, nearly without collision, as reported in [18]. The ionic species bombard the wafer surface perpendicularly, a demand for anisotropic etching [19].

The CCP power was set to 10 W for all experiments, as lower power values led to a steep decrease in etch rate. Similarly, the etch rate increases with the RF power on the ICP source, as shown in Fig. 2. The etch rate seems to saturate with ICP power above

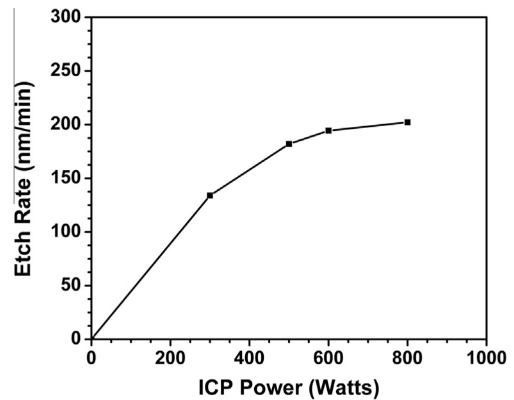

Fig. 2. Etch rate as a function of ICP power with $T = -90$ °C, 100 sccm SF_6 flow, and 5 sccm O_2 flow.

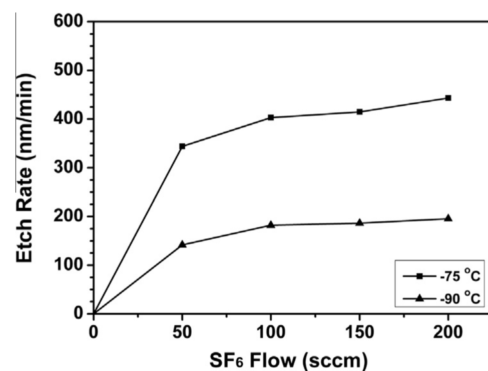

Fig. 3. Etch rate as a function of SF_6 flow with 5 sccm O_2 flow and 500 W ICP power.

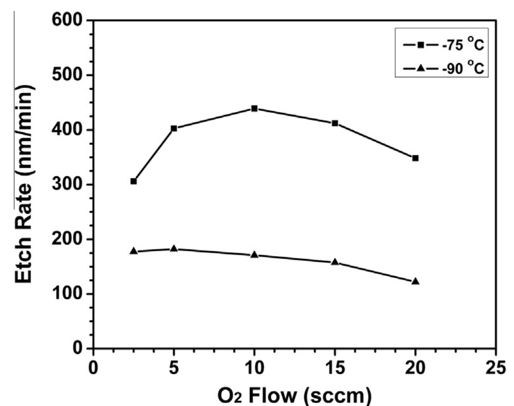

Fig. 4. Etch rate versus O_2 flow with 100 sccm SF_6 flow and 500 W ICP power.

500 W under these process conditions (see the figure caption). The observed saturation is due to the sheath layer in the chamber [20], and depends on the plasma density and hence, the SF_6 flow.

The effect of the SF_6 and O_2 flows is subsequently investigated with ICP RF power fixed at 500 W. Fig. 3 shows a sublinear monotonic increase in the etch rate with an increase in SF_6 flow for chuck temperatures of −75 °C and −90 °C. The etch rate is observed to increase very slowly beyond an SF_6 flow of 100 sccm.

The dependence of etch rate on oxygen flow is shown in Fig. 4. The etch rate at −75 °C shows an initial increase with oxygen flow which is attributed to the correlated increase in fluorine atom concentration [10–12,21]. A further increase in O_2 flow results in a decreased etch rate due to the dilution of reactive species beyond

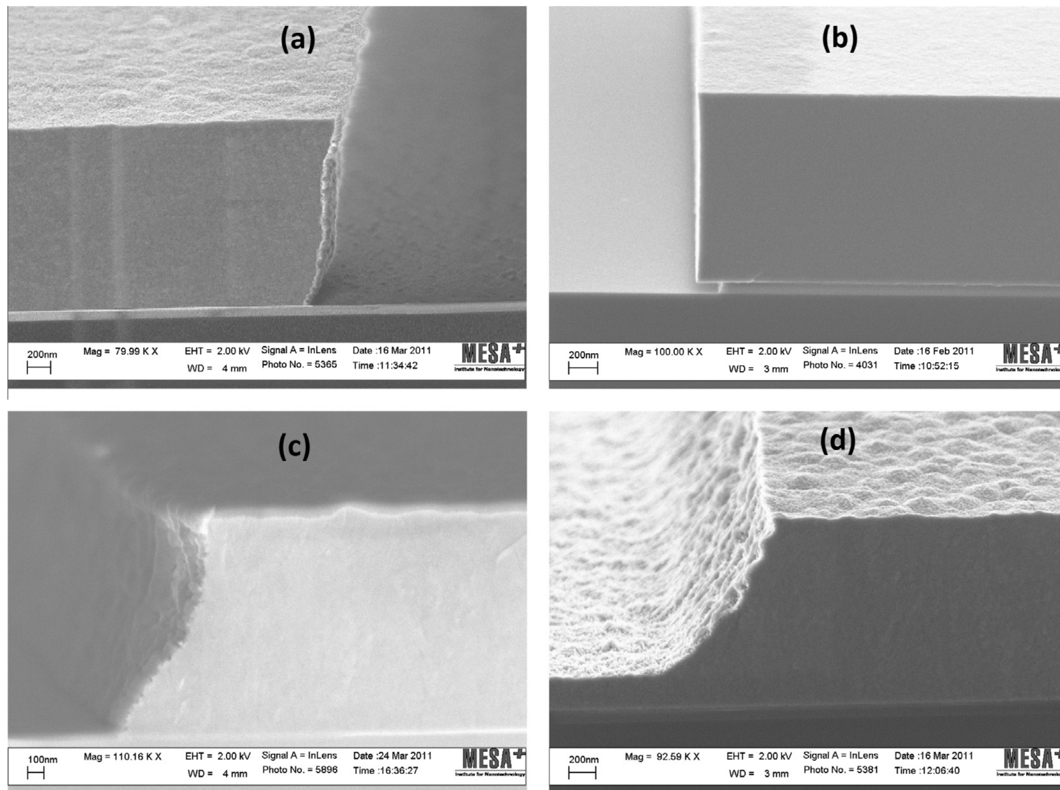

Fig. 5. Etch profiles for O_2 flow of (a) 2.5 sccm, (b) 5 sccm, (c) 15 sccm and (d) 20 sccm with 100 sccm SF_6 flow, $T = -90$ °C and 500 W ICP power.

Table 1
Etch recipes for vertical etching of highly B-doped $Ge_{0.7}Si_{0.3}$ and selectivity towards PECVD oxide.

SF_6 (sccm)	O_2 (sccm)	ICP (watt)	CCP (watt)	Pressure (mTorr)	He (mbar)	Temp. (°C)	Selectivity (GeSi:SiO_2)	Etch angle (°)
100	5	500	10	10	20	−90	35:1	90
100	5	500	10	10	20	−75	65:1	82
100	5	500	10	10	20	20	92:1	59

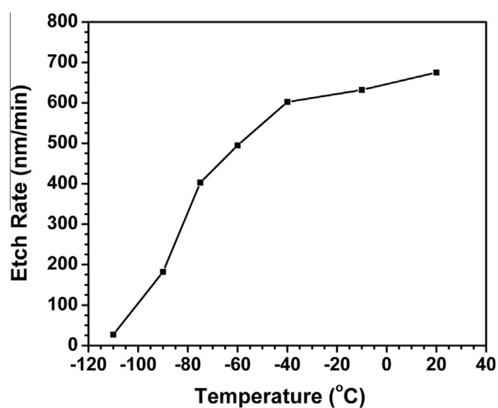

Fig. 6. GeSi etch rate as a function of chuck temperature with 100 sccm SF_6 flow, 5 sccm O_2 flow, and 500 W ICP power.

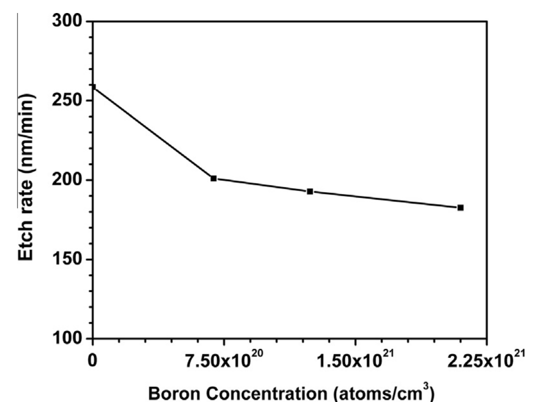

Fig. 7. Etch rate as a function of boron concentration in $Ge_{0.7}Si_{0.3}$ alloy with $T = -90$ °C, 5 sccm O_2 flow, 100 sccm SF_6 flow, and 500 W ICP power.

10 sccm; a similar trend is observed during the etching of Si [21]. The initial increase in etch rate is hardly visible in the −90 °C experiments.

The etch profile changes from a slightly negative taper at low oxygen flow, to positive taper as the oxygen flow is increased to 20 sccm: see Fig. 5 (for the −90 °C chuck temperature).The process parameters as detailed in Table 1 (first row) results in a vertical etch profile of highly doped $Ge_{0.7}Si_{0.3}$ alloy.

Fig. 6 shows the etch rate between −110 °C and 20 °C for a 20:1 SF_6:O_2 plasma at 13×10^{-3} mbar and CCP power of 500 W. The observed increase in etch rate with the increase of temperature is due to enhanced adsorption and reactivity of fluorine atoms with the etched material during DRIE, as also reported for Si etching [19].

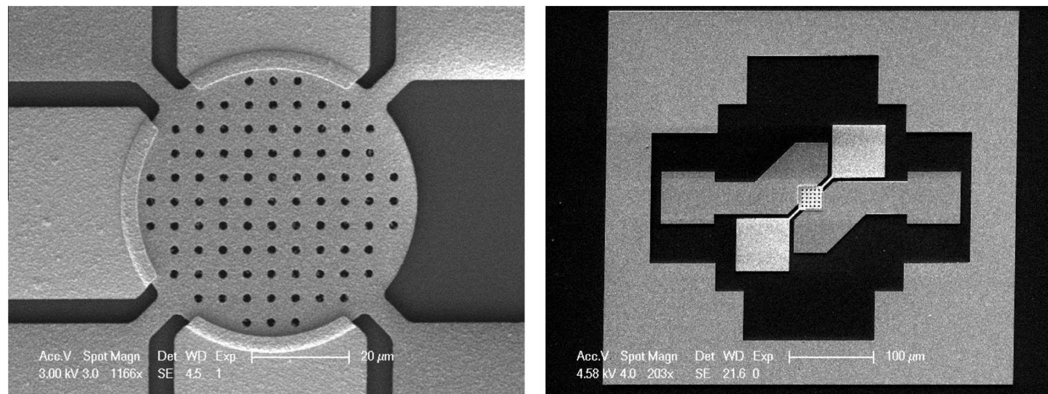

Fig. 8. Top-view SEM image of GeSi microresonators fabricated using the optimized etch results.

The etch selectivity towards plasma deposited SiO_2 is measured to be 35:1 at −90 °C, and even 65:1 at −75 °C chuck temperature. We find that the etch selectivity towards oxide increases further to 92:1 at 20 °C, but at the expense of an irregular etch profile due to the deposition of eroded photoresist on the side wall, as also reported for Si at 0 °C [19].

Fig. 7 shows the etch rate of $Ge_{0.7}Si_{0.3}$ alloy with varied boron concentration at process conditions indicated in the caption. The boron doped layers (6.9×10^{20} cm^{-3}) etch four times slower than the phosphorous doped silicon wafer ($\sim 1 \times 10^{15}$ cm^{-3}). The etch rate is found to decrease with an increase in the boron concentration. This decrease in the etch rate is caused due to increasing Coulomb repulsion between uncompensated boron (B^-) and fluorine ions (F^-), as explained by the space charge model of Lee et al. [12]. The obtained results are in line with the suppressed etch rate reported for p^+ doped silicon [22].

4. Micromachined GeSi resonators

With the optimized etch conditions, as listed in Table 1, poly $Ge_{0.7}Si_{0.3}$ micro-electromechanical resonators are fabricated, as shown in Fig. 8. Both the input/output electrodes, and the resonating structure with its anchors, are realized with GeSi material. The bottom layer (forming the resonating element) is etched at −90 °C, chosen for a vertical etch profile. The upper layer, defining the electrodes, is etched at a temperature of −75 °C for the higher selectivity towards the intermediate, thin silicon dioxide layer between the two $Ge_{0.7}Si_{0.3}$ layers. The fabricated resonator is fully functional, with Lamé mode resonance around 48 MHz [23].

5. Conclusions

We have reported on the reactive ion etching of highly boron doped $Ge_{0.7}Si_{0.3}$ layers in SF_6 and O_2 plasma using a Plasmalab 100 Plus system. The effects of RF power, SF_6 flow, O_2 flow and temperature on the etch rate in SF_6 and O_2 plasma are presented. The etch rate is strongly affected by the chuck temperature, less by the flow of SF_6 and O_2. The etch profile can be controlled with the oxygen concentration in the gas mixture. Selectivity towards PECVD silicon dioxide is 35:1 up to 92:1 at chuck temperatures of −90 °C and 20 °C respectively. The developed etch recipes are successfully employed in the fabrication of GeSi microresonators.

Acknowledgements

The authors would like to thank A. A. I. Aarnink and M. J. de Boer for their technical support. We also gratefully acknowledge I. -J. Holsema and M. A. Smithers from MESA+ Institute for Nanotechnology for their help in the cleanroom and SEM imaging, respectively. This work is financially supported by the Dutch Technology Foundation STW through project Grant No. 10048.

References

[1] H.V. Schreiber, B.G. Bosch, IEDM Tech. Dig. (1989) 27.2.1–27.2.4.
[2] C. Salm, D.T. van Veen, D.J. Gravesteijn, J. Holleman, P.H. Woerlee, J. Electrochem. Soc. 144 (1997) 3665–3673.
[3] T. Ghani et al., IEDM Tech. Dig. (2003) 978–980.
[4] J. Zimmer, H. Stiebig, H. Wagner, J. Appl. Phys. 84 (1998) 611–617.
[5] M.V. Kumar, V. Subramanian, K.C. Saraswat, J.D. Plummer, W. Lukaszek, Proc. Int. Conf. Microelectron. Test Struct. 10 (1997) 143–145.
[6] T.J. King, R.T. Howe, S. Sedky, G. Liu, B.C.Y. Lin, M. Wasilik, C. Duenn, Dig. Int. Electron. Device Meet. (2002) 199–202.
[7] M. Gromova et al., Proc. 20th IEEE Int. Conf. on MEMS (2007) 759–762.
[8] L. Guo, K. Li, D. Liu, Y. Ou, J. Zhang, Q. Yi, S. Xu, J. Cryst. Growth 227–228 (2001) 801–804.
[9] M.C. Peignon, C. Cardinaud, G. Turban, C. Charles, R.W. Boswell, J. Vac. Sci. Technol. A14 (1996) 156–164.
[10] Y. Zhang, G.S. Oehrlein, E. de Fresart, J. Vac. Sci. Technol. A 5 (11) (1993) 2492–2495.
[11] Y. Zhang, G.S. Oehrlein, E. de Fresart, J.W. Corbett, J. Appl. Phys. 71 (1992) 1936–1942.
[12] Y.H. Lee, M.-M. Chen, A.A. Bright, Appl. Phys. Lett. 46 (1985) 260–262.
[13] J.W. Bartha, J. Greschner, M. Puech, P. Maquin, Proc. Micro Nano Eng. 27 (1995) 453–456.
[14] S.N.R. Kazmi, A.Y. Kovalgin, A.A.I. Aarnink, C. Salm, J. Schmitz, ECS J. Solid State Sci. Technol. 1 (5) (2012) P222–P226.
[15] T.D. Bestwick, G.S. Oehrlein, Y. Zhang, G.M.W. Kroesen, Appl. Phys. Lett. 59 (3) (1991) 336–338.
[16] D. Dries, European Patent No. 2025775 (2009) A1.
[17] H. Jansen, H. Gardeniers, M. de Boer, M. Elwenspoek, J. Fluitman, J. Micromech. Microeng. 6 (1996) 14–28.
[18] A. Manenschijn, W.J. Goedheer, J. Appl. Phys. 69 (1991) 2923–2930.
[19] M.J. de Boer, J.G.E. Gardeniers, H.V. Jansen, E. Smulders, M.-J. Gilde, G. Roelofs, J.N. Sasserath, M. Elwenspoek, J. Microelectromech. Syst. 11 (2002) 385–401.
[20] A.A. Ehsan, S. Shaari, B.Y. Majlis, Int. Conf. Semicond. Electron. (2000) 228–230.
[21] H. Zou, Microsyst. Technol. 10 (2004) 603–607.
[22] L. Baldi, D. Beardo, J. Appl. Phys. 57 (1985) 2221.
[23] S.N.R. Kazmi, A.A.I. Aarnink, C. Salm, J. Schmitz, Int. Freq. Control Symp. (2012), http://dx.doi.org/10.1109/FCS.2012.6243633.